Spectroscopic study of jet-cooled fluoranthene

I. Y. Chan and Marcos Dantus
Department of Chemistry, Brandeis University, Waltham, Massachusetts 02254

(Received 26 November 1984; accepted 11 February 1985)

Fluorescence excitation and single vibronic level (SVL) fluorescence spectra of fluoranthene seeded in an Ar free-jet are presented. The S_1 excitation spectrum builds on a strong 427 cm^{-1} vibronic false origin. Fluorescence spectra exciting SVL with vibrational energy 0, 427, and 751 cm^{-1} contain sharp lines, whereas with 1345 cm^{-1} the fluorescence spectrum is a featureless continuum. The sharp lines have been analyzed and assigned with the help of Raman and IR data. The broad spectrum when exciting 1345 cm^{-1} above the S_1 origin is ascribed to energy redistribution (IVR). The behavior of fluoranthene in light of current understanding of the IVR process is discussed.

I. INTRODUCTION

Fluoranthene is a much studied nonalternant aromatic hydrocarbon. Its formal structure suggests a phenyl moiety strongly coupled to a naphthalene nucleus, see Fig. 1. In a series of publications reporting semiempirical calculations, polarized spectroscopy, and MCD results, Michl and coworkers have demonstrated that the above simplistic picture is incorrect.[1] The fluoranthene framework has to be considered in its totality; from such treatments many electronic transitions are predicted in the UV region. Especially, three electronic transitions were established in the 300–400 nm wavelength region, with a S_1–S_2 separation of only approximately 2500 cm^{-1}.[1] In photophysics, fluoranthene is noted to exhibit dual fluorescence in the condensed phase, a clear-cut exception to Kasha's rule.[2] Current wisdom attributes this behavior to a (strong) coupling between two electronic states with very small energy spacing.[2] Quantitative interpretation of photophysical results, however, has been hampered by the imprecision of spectroscopic data. The $S_1 \leftarrow S_0$ transition, of the ^1L_b type, appears as very weak shoulders to the much stronger $S_2 \leftarrow S_0$ transition in conventional spectroscopy. Indeed, the absorption band is so inconspicuous that Michl *et al.* had to argue carefully to establish its existence.[1] The only high resolution spectroscopy work to date is an early study conducted in a Shpolskii matrix.[3] This early investigation was mainly an attempt to correlate the vibrational frequencies of fluoranthene with those of naphthalene and benzene. The appropriateness of this approach is debatable in view of the present understanding of the electronic structure of fluoranthene.[1] Furthermore, this previous work provides only the most qualitative information concerning spectral intensity. As such, it is useless for, say, estimating radiative lifetime of the S_1 state. In this article we present a thorough supersonic-jet spectroscopic study of the S_1 state of fluoranthene. Where the scope of our investigation overlaps with that of Pesteil *et al.*,[3] we provide an interesting comparative study. In addition, our results on resolved fluorescence after single-vibronic-level (SVL) excitation shed some light on intramolecular vibrational energy redistribution (IVR) in fluoranthene.

II. EXPERIMENTAL

Fluoranthene (Aldrich 98%) was recrystallized in ethanol before use. The supersonic valve, capable of operating at over 400 °C, was a modified Bosch design developed by Cheng in this laboratory. Nozzle diameter was either 0.25 or 0.5 mm. In a typical experiment, a 6 in. diffusion pump maintained a pressure of less than 10 μ for repetition rates up to 10 Hz in a free-jet expansion. A Molectron nitrogen laser (UV 22) pumped a dye laser (DL200) with resolution of 1.3 cm^{-1}. Three dyes (PBBO, BBQ, and PBD) covered the wavelength range of our interest. Fluorescence was detected with a selected Hamamatzu R928P photomultiplier feeding into a PAR 162/164 Boxcar Integrator. For dispersed fluorescence spectra, we used a 3/4 M monochromator (Spex 1702) with a dispersion of 4.4 Å/mm operating in the tenth order. All fluorescence spectra have a slit resolution of ~13 cm^{-1}. Unfortunately, stringent order-sorting requirements limited the wavelength range of our spectra. Published spectra are the sum of 4–10 scans using a Fabri-Tek 1062 signal averager, the output of which were digitized for further data

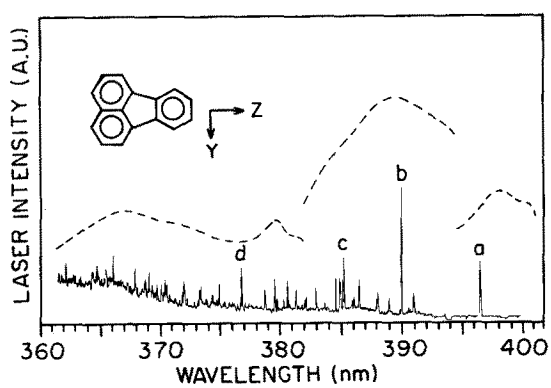

FIG. 1. Fluorescence excitation spectrum of the S_1 state of fluoranthene. Line intensity is not corrected for laser power variations, but such variations are plotted in the figure. The four lines upon which resolved fluorescence are presented in Fig. 3a, b, c, and d and are labeled a, b, c, and d, respectively. Nozzle temperature 150 °C, $x/d = 36$, $P_0 = 10$ psig. Laser linewidth = 1.3 cm^{-1}.

 0021-9606/85/114771-06$02.10

processing. Laser and the monochromator wavelengths were periodically calibrated with a Hg spectral lamp.

III. RESULTS AND DISCUSSIONS

Supersonic expansion was performed with argon as carrier gas. A stagnant pressure of 10 psig was found to optimize the signal from the cold molecules. For excitation spectroscopy the source temperature was kept at 150 °C. For dispersed fluorescence experiments we ran at temperatures up to 220 °C in order to increase the signal. No signs of condensation or dust particle formation were evident even at the highest temperature. All data reported were obtained with 9 mm distance to the jet, thus $X/D = 36$. No van der Waals complexes were observed under our experimental conditions.

A. Fluorescence excitation spectrum

We present a condensed fluorescence excitation spectrum of fluoranthene in Fig. 1. The peak intensity is not corrected for variation of laser power, but the relative power curve of the three dyes measured during data collection is plotted in the figure. The line marked "a" is the origin. No other signals were observable at longer wavelengths for several hundred cm^{-1}. It is located at 25 216.9 cm^{-1} (air). In the only high resolution work published to date, Pesteil *et al.* reported many Shpolskii multiplets in the origin region.[3] The value they used for vibrational analysis (the "$n = 3$" component) may be calculated to be at 24 516 cm^{-1}. Thus the matrix spectrum in *n*-pentane has a red shift of 700 cm^{-1} from the gas phase value. In all, nearly one hundred vibronic bands have been observed. Below 370 nm, a broad underlying background is evident. This is only partly due to spectral congestion in the region. Most likely, it is ascribed to the hot bands of the much stronger $S_2 \leftarrow S_0$ transition due to the small fraction of vibrationally hot molecules. Such background is much more prominent on experiments with lower X/D values.

The spectral data are given in Table I. The wavelengths, relative position, intensity, and analysis have their usual meaning. In column 4 we list some of the vibronic bands reported by Pesteil *et al.*[3] which we correlate to our results. Only for 11 out of their 19 reported frequencies we managed to make such a correlation. For these lines the difference is of the same sign (red shifted in matrix) and similar magnitude (18–25 cm^{-1}). This pattern may be rationalized by lattice participation in the reduced-mass and/or force constants. It is noteworthy that some of the stronger bands in Ref. 3 (277, 1194 cm^{-1}) do not find their counterparts in our much more detailed spectrum. The reason for this observation is not clear.

For such a large molecule posessing only C_{2v} symmetry to first order, a complex spectrum is to be expected. The spectrum, however, is quite interpretable. It features a strong vibronic band (427 cm^{-1}) which serves as a false origin; combinations containing the 427 cm^{-1} mode carry more than half the vibronic intensity. In addition, a large number (29) of combinations involve the frequency 386 cm^{-1}. This mode by itself is quite weak, but it brings in about one-third the vibronic activities through combinations. Based on its low frequency and weak dipole strength, one may speculate that it is an out-of-plane mode of $A_2 = B_2 \times b_1$ vibronic symmetry. (See next paragraph for electronic symmetry assignment.) The alternative of Franck–Condon forbiddenness seems unlikely in view of the absence of simple overtones. In all, a total of 21 vibrational modes are directly observed, and 23 modes are further deduced through combinations.

In a series of extensive work, Michl and co-workers[1] established the nature of the various excited states of fluoranthene, without paying attention to the symmetry species of any states. For our subsequent presentation it is convenient to deduce such symmetry here. In an axis in which the twofold axis is z and the in-plane short axis is y, the first absorption band is y polarized while the second band is z polarized. Furthermore, PPP calculations established the predominant configuration for S_1 and S_2 to be $F_2 \rightarrow F_{-1}$ and $F_1 \rightarrow F_{-1}$, respectively (other configurations have the same symmetry). The one-electron orbitals F_1, F_{-1}, and F_2 possess a_2, a_2, and b_1 symmetry, respectively.[1] All these information lead to assignment of electronic symmetry B_2 for S_1 and A_1 for S_2. This assignment is most helpful in interpreting our observed excitation spectrum. The $S_1 \leftarrow S_0$ origin is symmetry allowed ($^1B_2 \leftarrow {}^1A_1$) but lacks intensity due to its ^1L_b nature. The false origin at 427 cm^{-1} derives its dipole strength through vibronic coupling of S_1 to S_2. Under this scheme, the 427 cm^{-1} mode belongs to an in-plane vibrational species b_2.

A historical comment may be appropriate in the present context. Among the vibronic bands reported by Pasteil *et al.*[3] which are identified in Table I, most of them are combination bands. Since these frequencies do not represent individual vibrational modes, it is impossible to seek their correlation with benzene or naphthalene modes. Regardless of whether the molecule-in-molecule model is valid for fluoranthene, Pasteil *et al.* had embarked on a futile effort.

B. Fluorescence spectrum from the origin

Low temperature fluorescence spectrum of fluoranthene extends over a wide wavelength range. Even after ignoring the $S_2 \rightarrow S_0$ contribution, the fluorescence persists for nearly 7000 cm^{-1}. This behavior has been taken by Berlman *et al.*[4] as indication that the S_1 state may be nonplanar. Such extended emission spectrum has been observed also in the present work, with the low energy part congested into a featureless continuum (see Fig. 4). The higher energy portion of the spectrum is well resolved. We present a section of the emission spectrum by exciting the origin of the S_1 in Fig. 2. It is unfortunate that such a low branching ratio is translated into a very long data acquisition process.

Our analysis of fluorescence spectra is facilitated by the recent work of Klaeboe *et al.*[5] who reported Raman, IR, and far IR spectra of fluoranthene along with a normal mode analysis. In Table II we list the spectral information concerning Fig. 2. Under the column marked Klaeboe we give the Raman or IR frequencies observed by them. Many modes were observed by both techniques in their paper, with frequencies agreed to within 6 cm^{-1}. In order to save space only the number from the stronger spectral band is listed

TABLE I. Fluorescence excitation spectrum analysis.

Wavelength (Å)	Shift[a] (cm^{-1})	Rel. int.	Pesteil[b] (cm^{-1})	Analysis	Wavelength (Å)	Shift[a] (cm^{-1})	Rel. int.	Pesteil[b] (cm^{-1})	Analysis
3965.6	0	45		Origin (a)[c]	3794.9	1134	7		386 + 2(374)
3935.6	192	2			3793.2	1146	18	1119	2(386) + 374
3090.8	360	8			3792.2	1153	8		427 + 726
3909.0	365	11							427 + 3(241)
3905.8	386	2			3784.1	1207	13	1194	
3904.3	396	3			3764.8	1345	23	1325	862 + 483(d)
3899.5	427	72	408	(b)					968 + 377
3897.1	433	3			3763.9	1351	6		386 + 3(322)
3888.2	502	10			3757.6	1396	5		427 + 4(241)
3879.1	562	12	547	427 + 135	3757.0	1400	4		427 + 3(324)
3879.0	563	11			3745.6	1481	12	1457	386 + 322 + 775
3878.1	569	8		sequence					386 + 374 + 721
3877.2	575	3							778 + 703
3863.2	668	17	650	427 + 241	3741.3	1510	5		386 + 3(374)
3862.2	675	3			3739.7	1523	6		862 + 661
3859.1	696	7		427 + 2(135)	3730.6	1588	10	1569	427 + 726 + 435
3857.6	706	5		386 + 322	3729.0	1600	8		386 + 2(322) + 572
3850.9	751	30	720	427 + 324(c)	3718.7	1674	5		386 + 4(322)
3849.6	760	18		386 + 374					2(386) + 374 + 528
3847.6	773	17			3716.8	1688	9		
3846.9	778	19			3716.1	1693	14		427 + 2(241) + 783
3844.1	797	19							427 + 726 + 540
3834.5	862	5			3714.8	1702	8		
3827.5	910	12		427 + 2(241)	3712.1	1722	3		968 + 2(377)
3819.0	968	8	951		3704.1	1780	5		386 + 4(322) + 106
3818.3	973	6		sequence	3702.1	1795	10		
3817.2	980	5			3701.4	1800	9		2(386) + 374 + 654
3815.0	995	3							386 + 4(322) + 126
3810.2	1028	11		386 + 2(322)	3700.6	1806	13		386 + 3(322) + 455
3804.0	1071	3			3699.5	1814	5		386 + 3(714)
3803.6	1074	15	1056	427 + 2(324)	3967.4	1829	10		862 + 2(483)
3799.8	1100	5		386 + 714	3693.9	1855	9		
3691.8	1870	5			3629.2	2337	6		
3690.6	1879	4		427 + 2(726)	3625.2	2368	6		
3689.6	1886	8		386 + 4(322) + 2(106)	3623.3	2382	7		
					3622.1	2391	4		
3686.8	1907	15		3(386) + 2(374)	3617.4	2427	13		
3683.9	1928	10		386 + 2(322) + 572 + 328	3613.9	2454	7		2(386) + 374 + 2(654)
				386 + 4(322) + 2(126)	3613.1	2460	4		427 + 3(241) + 3(435)
3683.0	1935	8			3611.0	2476	8		427 + 2(241) + 2(783)
3677.1	1978	5		968 + 2(377) + 256					
3675.3	1992	15		386 + 4(322) + 3(106)					
3674.2	2000	3							
3670.9	2024	5		427 + 726 + 2(435)					
3668.6	2041	7							
3661.0	2098	4		386 + 4(322) + 4(106)					
3657.2	2126	18							
3651.1	2172	7		386 + 2(322) + 2(572)					
3650.4	2177	10							
3649.5	2184	5		778 + 2(703)					
				862 + 2(661)					
3647.0	2203	4		386 + 374 + 2(721)					
				2(386) + 374 + 2(528)					
3644.8	2219	5							
3642.9	2234	9		2(427) + 3(241) + 2(540)					
				968 + 2(377) + 2(256)					
3639.9	2256	9		386 + 2(322) + 572 + 2(328)					
				386 + 322 + 2(775)					
3639.3	2261	8		386 + 3(322) + 2(455)					
3636.8	2280	4							

[a] Relative energy from the origin.
[b] Reference 3.
[c] a, b, c, and d refer to indices in Fig. 1.

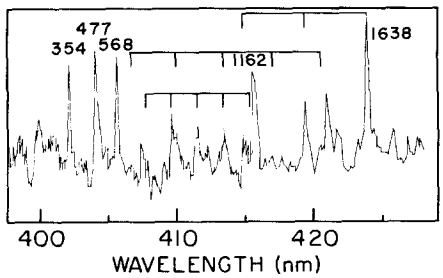

FIG. 2. Fluorescence spectrum from the S_1 origin. Intensity is not corrected for the S-20 cathode response. The true origin is avoided in our experiment due to interference from scattered light. Slit resolution = 13 cm^{-1}. Nozzle temperature = 220 °C, $x/d = 36$, $P_0 = 10$ psig.

here. We also attach their symmetry assignment for the various modes for reference.

The following comments on this spectrum may be interesting. (1) The spectrum is relatively clean and straightforward to interpret. Only the mid-wavelength range (406–415 nm) contains a series of weaker and broader features. These features may be accounted for by two progressions riding on the 622 and 699 cm^{-1} modes. (2) The correlation between our vibronic bands and those reported by Pesteil *et al.*[3] are more satisfactory than in the excitation spectrum (cf. Table I). Most modes are identified, and the difference between the two sets of reported frequencies are much smaller ($\sim \pm 3$ vs ~ 20 cm^{-1}). This larger shift of vibrational frequencies in the S_1 compared to that of the S_0 state is consistent with the general trend that an excited state is more polarizable by the medium than the ground state. (3) In subsection A we have deduced that the S_1 and S_2 have B_2 and A_1 symmetry, respectively. Under this assignment fluorescence from the origin of S_1 may have intensity to a_1, a_2, and b_2 modes, whereas emission to a b_1 mode in the ground manifold is symmetry forbidden. An examination of Table II indicates only two possible b_1 modes as assigned by Klaeboe *et al.*: 355 b_1 and 804 a_1/b_1. The latter is a weak peak, and Klaeboe's assignment is ambivalent. The 354 cm^{-1} peak is strong in our spectrum. However, a close look at Ref. 3 indicates the observed Raman peak may be assigned either as b_1 (319 cm^{-1}) or b_2 (396 cm^{-1}) based on their calculations. Therefore it need not be a serious objection. In summary, the assignment of the fluorescence bands is quite consistent with the electronic symmetry.

C. Fluorescence from higher SVL's

In Fig. 3 we present several fluorescence spectra after single vibronic level (SVL) excitation. For comparison the origin emission shown in Fig. 2 is also included. The spectral resolution is 13 cm^{-1}. The excitation wavelength for each spectrum is indicated by an arrow. As this wavelength gets shorter, there is an increase in the underlying continuum. This is an instrumental artifact, probably due to fluorescence

TABLE II. 0°-level fluorescence assignments.

Wavelength (Å)	Shift[a] (cm^{-1})	Rel. int.	Pesteil[b] (cm^{-1})	Klaeboe[c] (cm^{-1})	Combination
4022	354	34	352	$355b_1$	
4042	477	38	474	$477a_1$	
4057	568	37	565	$564a_2$	
			607		
4066	622	4			
4074	671	11	673	$672a_1$	
4079	699	7			
			763		
4097	809	20	802	$804a_1/b_1$	699 + 110
4100	827	14			622 + 204
4116	919	17	917	$910a_2$	699 + 2(110)
4123	964	10	960	$970a_1$	
			1017		
4135	1031	16	1039	$1038b_2$	699 + 3(110)
					622 + 2(204)
4148	1110	14	1106	$1103a_1$	
4154	1144	12			699 + 4(110)
4157	1162	32	1159	$1159b_2$	
4170	1235	12		1228	622 + 3(204)
			1279		
			1293		
4183	1313	8			
4194	1374	18	1370		1110 + 264
4206	1441	10	1432	$1439b_2$	622 + 4(204)
4210	1463	27	1463	$1459a_1$	
4216	1499	16	1494		
4234	1599	10	1612	1599	
4241	1638	44		1632	1110 + 2(264)
4259	1739	12		1735	

[a] Relative energy from the origin.
[b] Reference 3.
[c] Reference 5.

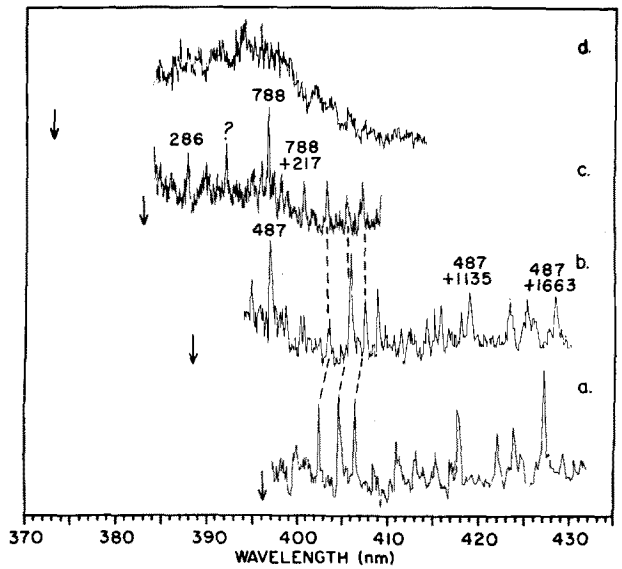

FIG. 3. Resolved fluorescence after exciting various SVL's. The SVL's have vibrational energy 0, 427, 751, and 1345 cm^{-1} in a, b, c, and d, respectively. Operational conditions same as in Fig. 2. A few modes which are active in several spectra are linked by broken lines.

from the order-sorting filter, since a similar continuum is absent in a preliminary low-resolution scan in first order (see Fig. 4). Figure 3d, corresponding to 1345 cm^{-1} in vibrational energy, is distinctly different from the other spectra. While some peaks are descernible above the background continuum, they are too weak and too numerous for detailed measurement. The stronger peaks for Figs. 3b and 3c are listed in Table III.

Figure 3b is the fluorescence spectrum after exciting the strong false origin with 427 cm^{-1} vibrational energy. It thus offers an opportunity to learn more about the promoting mode. The only strong peak in Fig. 3b occurring slightly to the red of the S_1–S_0 origin is at 397.5 nm, which is presumably the ν_1^1 type sequence band. The ground state frequency of the promoting mode is therefore 487 cm^{-1}. A look at Ref. 3 does find a mode at 487 cm^{-1}, which was observed in Raman, IR, and far IR. This gratifying consistency is marred

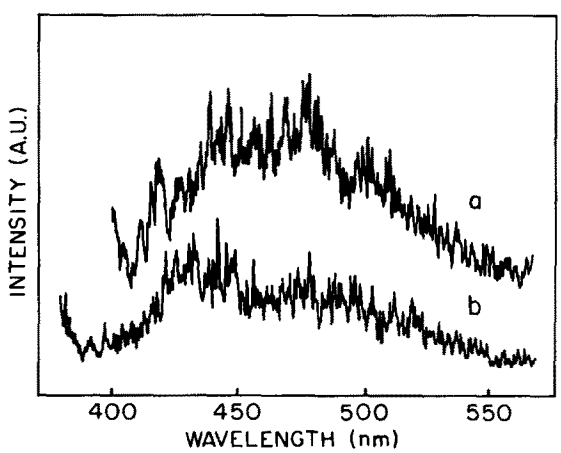

FIG. 4. Low resolution fluorescence spectra. Vibrational energy in a and b is 0 and 1345 cm^{-1}, respectively. Slit resolution = 3.3 nm. Other operational conditions same as in Fig. 2.

TABLE III. Stronger fluorescence lines exciting higher SVL's.

Wavelenth (Å)	Shift[a] (cm^{-1})	Rel.[b] int.	Analysis	Klaeboe[c] (cm^{-1})
		Exciting the 427 cm^{-1} band		
3975	487	60	487	$487a_2$
3998	629	12	487 + 142	$140a_2$
4003	662	22	487 + 175	172
4007	687	22	487 + 200	$203b_2$
4032	840	19	487 + 2(175)	
			487 + 353	$355b_1$
4052	964	54	487 + 474	$475a_1$
4066	1051	30	487 + 564	$564a_2$
4079	1127	35	487 + 640	$637a_2$
4097	1238	12	487 + 751	$750b_2$
4107	1296	8	487 + 809	$804a_1/b_2$
4110	1312	10	487 + 827	$827b_1$
4125	1404	19	487 + 917	913
4133	1451	25	487 + 964	$969b_1$
4139	1484	26	487 + 997	$994b_1$
4146	1526	15	487 + 1039	$1038b_2$
4159	1598	25	487 + 1111	
4163	1622	30	487 + 1135	$1136a_1$
4177	1702	8	487 + 1215	1217
4190	1777	8	487 + 1290	1291
4209	1884	23	487 + 1397	1396
4227	1986	25	487 + 1499	
4232	2017	16	487 + 1530	1529
4249	2110	11	487 + 1623	1621
4256	2150	26	487 + 1663	1660
		Exciting the 751 cm^{-1} band		
3860.4	64	55	64	68
3866.4	104	42	104	106
3893.8	286	50	286	286
3911.6	403	40	403	$407b_2$
3931.1	530	57	?	
3965.0	747	40	747	$746b_2$
3969.7	777	32	777	$775b_1$
3971.4	788	83	487 + 301[d]	$305a_1$
3983.6	865	30	788 + 77	79
4000.2	969	15	788 + 181	$180b_1$
4005.9	1005	38	788 + 217	
4028.1	1142	38	788 + 354	$355b_1$
4047.6	1262	25	788 + 474	$475a_1$
4060.4	1340	22	788 + 552	$556b_1$
4063.1	1356	36	788 + 568	$564a_2$
4080.3	1460	25	788 + 672	$675a_1$

[a] Relative energy from the 0_0 of the S_0.
[b] Only stronger lines are listed.
[c] Reference 5. In case of combinations, only the additional mode is listed.
[d] The 751 cm^{-1} line in the excitation spectrum is assigned 427 + 324. If so the corresponding assignment here is as shown.

by Klaeboe's assignment of this mode to a_2, based on the proximity of a calculated frequency. We, however, find this a_2 assignment troublesome. As the S_1 and S_2 are established (see Sec. III A) to be of B_2 and A_1 symmetry, respectively, the promoting mode connecting these two states via Herzberg Teller coupling should be of b_2 symmetry. Moreover, an a_2 mode should not be IR active, contrary to their IR and far IR observation. We can only speculate on the origin of this major discrepancy. Conceivably, since the promoting mode is one along which the electronic energy is very sensitive, conventional force-field calculations may not represent the b_2 promoting mode realistically.

With the 487 cm^{-1} mode identified, the rest of the 427 cm^{-1} SVL fluorescence bands are easily assigned. Most of the stronger peaks are combinations riding on the 487 cm^{-1}

sequence band serving as false origin. Under this interpetation, one may expect vibronic activities in this spectrum similar to those exhibited in the origin fluorescence. It is gratifying to observe that many modes, notably the strong triplet at 354, 477, and 568 cm^{-1}, are found common to both spectra. In a similar fashion, most of the stronger bands in Fig. 3c are assignable. The peaks to the red of the S_1 origin may be interpreted as combinations building on the sequence band at 788 cm^{-1}. Furthermore, the same triplet is once again prominent. In summary, spectroscopic analysis indicates that S_1 fluorescence with vibrational energy up to 751 cm^{-1} is mainly (if, not completely) resonance in nature.

The same can not be said with vibrational energy of 1345 cm^{-1}, where, as shown in Fig. 3d, the spectrum is devoid of any strong sharp peaks. We believe this is a demonstration of intramolecular energy flow (IVR) in fluoranthene. Figure 3d, unfortunately, is heavily obscured by an underlying background. Since no sharp peaks are to be seen we present some low resolution spectra over a wide wavelength range in order to gain some perspective. They were obtained on a Jarrell–Ash 1/4 M monochromater in the first order without any prefiltering. Figures 4a and 4b are fluorescence spectra exciting the origin and the 1345 cm^{-1} band, respectively. The slit resolution is 3.3 nm. At the beginning of each trace there is some intensity ascribed to scattered light, but the underlying background so prominent in Fig. 3d is now absent. Although at much poorer resolution, the spectral features in Fig. 2 are reproduced in the short wavelength section of Fig. 4a. Furthermore, the Franck–Condon profile of Fig. 4a is consistent with the published low temperature fluorescence spectrum.[2] Now Fig. 4b shows an onset of intensity near the $S_1 \rightarrow S_0$ origin, and it gradually gains strength up to the Franck-Condon maximum. This behavior, parallel to that of origin fluorescence, coupled with the absence of sharp lines in the short wavelength region, indicates that vibrational energy has undergone redistribution before emission could take place.

Dispersed fluorescence after SVL excitation of a jet-cooled molecule has been extensively used to investigate the IVR process in the S_1 state.[6–8] As a general trend, fluorescence from SVL with low vibrational energy is resonance in nature, with sharp and assignable vibrational structures. Emission after exciting a high vibronic state, typically with 2000 cm^{-1} or more vibrational energy, consists of broad bands weakly redshifted from the origin emission but showing similar intensity distribution. These broad bands are emitted by a large number of combination states populated through the IVR process. In the intermediate energy range, state-specific behavior has been reported with the IVR rate fluctuating up to a factor of 100.[7] The spectra resembles the origin emission but may exhibit complicated structures. In fluoranthene, SVL's with vibrational energy of 0, 427, and 751 cm^{-1} exhibit resonance fluorescence, as might be expected. Exciting the level with 1345 cm^{-1} vibration energy, however, gives rise to a fluorescence spectrum which suggests complete vibrational relaxation before emission. Thus the "high energy" range starts at 1345 cm^{-1} (or lower) in fluoranthene. This is one of the lowest values reported for the "statistical" behavior, all the more impressive since larger molecules like tetracene and perylene enter this high energy regime only at substantially higher vibrational energy. Perhaps the longer fluorescence lifetime and the lower molecular symmetry of fluoranthene account for the difference in behavior. In this context, it will be interesting to investigate the evolution of IVR behavior in the vibrational energy range 750–1345 cm^{-1}. Conceivably fluoranthene may exhibit a distinct pattern of activities in this intermediate energy range. Unfortunately the extremely unfavorable branching ratio of fluoranthene fluorescence (cf. Fig. 4) will imply a monumental effort in its execution.

ACKNOWLEDGMENTS

We are most grateful to Andrew Lap-tak Cheng, who developed the high-temperature pulse valve. This work is supported in part by the NSF (CHE-8113452) and by the Agricultural University of Wageningen (The Netherlands). One of us (M.D.) is grateful for the support of the Undergraduate Research Program of the Brandeis University.

[1] E. Heilbronner, J. P. Weber, J. Michl, and R. Zahradnik, Theor. Chim. Acta (Berl.) **6**, 141 (1966); J. Michl, J. Mol. Spectrosc. **30**, 66 (1969); J. Kole, E. K. Thulstrup, and J. Michl, J. Am. Chem. Soc. **96**, 7188 (1974).
[2] D. L. Philen and R. M. Hedges, Chem. Phys. Lett. **43**, 358 (1976), and earlier references cited therein.
[3] L. Pesteil, P. Pesteil, and F. Laurent, Can. J. Chem. **42**, 2601 (1964).
[4] I. B. Berlman, H. O. Wirth, and O. J. Steingraber, J. Am. Chem. Soc. **90**, 566 (1968).
[5] P. Klaeboe, S. J. Cyvin, A. P. Asbjornsen, and B. N. Cyvin, Spectrochim. Acta Part A **37**, 655 (1981).
[6] R. E. Smalley, J. Phys. Chem. **86**, 3504 (1982), and earlier references cited therein.
[7] C. Bouzou, C. Jouvet, J. B. Leblond, Ph. Millie, and A. Tramer, Chem. Phys. Lett. **97**, 161 (1983); S. A. Schwartz, and M. R. Topp, Chem. Phys. **86**, 245 (1984).
[8] W. R. Lambert, P. M. Felker, and A. H. Zewail, J. Chem. Phys. **81**, 2209 (1984).